Field limit and
nano-defects covering material surface
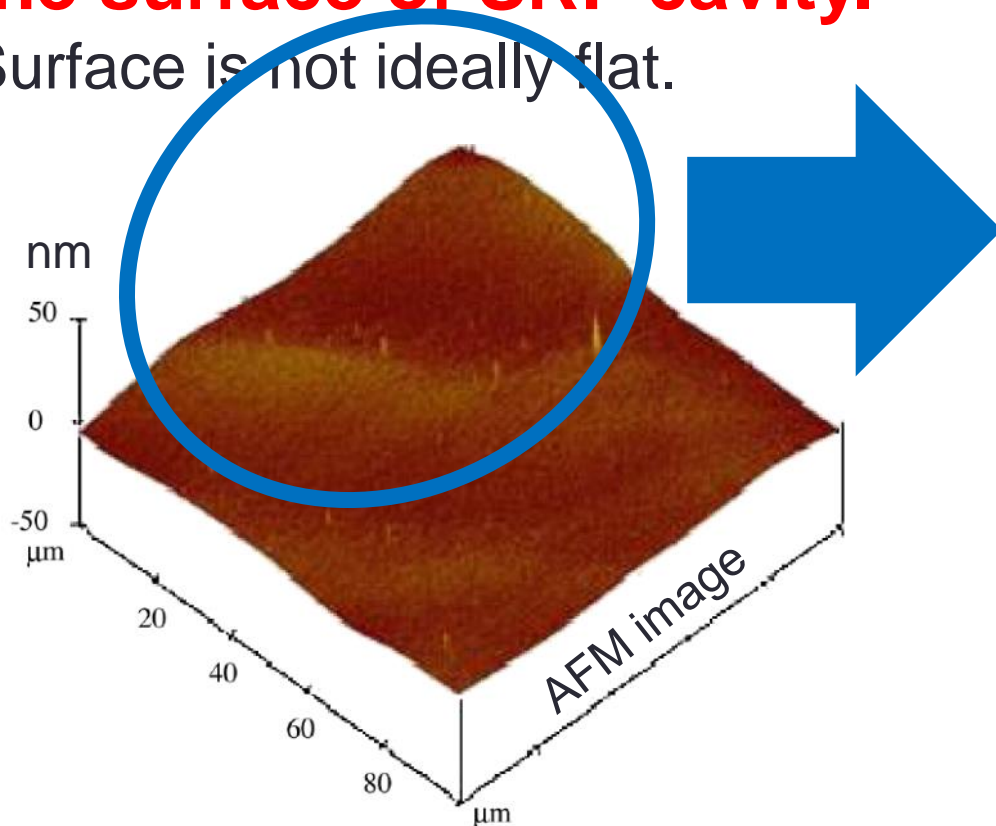
KEK

Takayuki KUBO

**TESLA Technology Collaboration meeting,
KEK, Tsukuba, Japan (2014)**
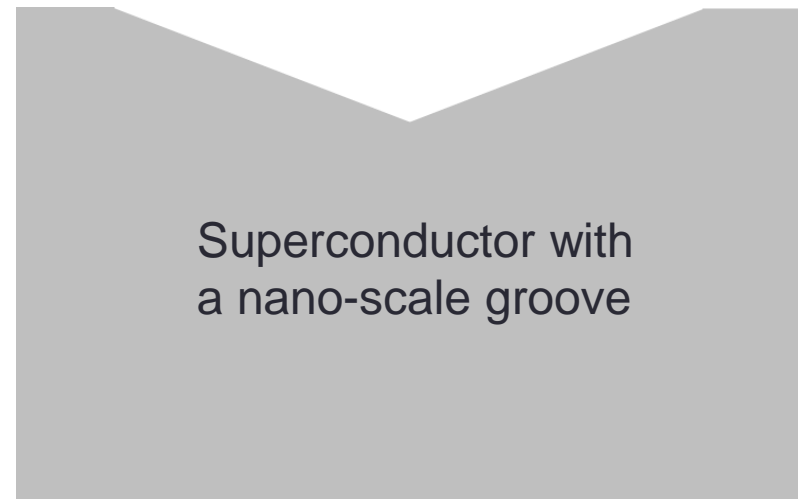
Nano-scale defects almost continuously distribute on the surface of SRF cavity.
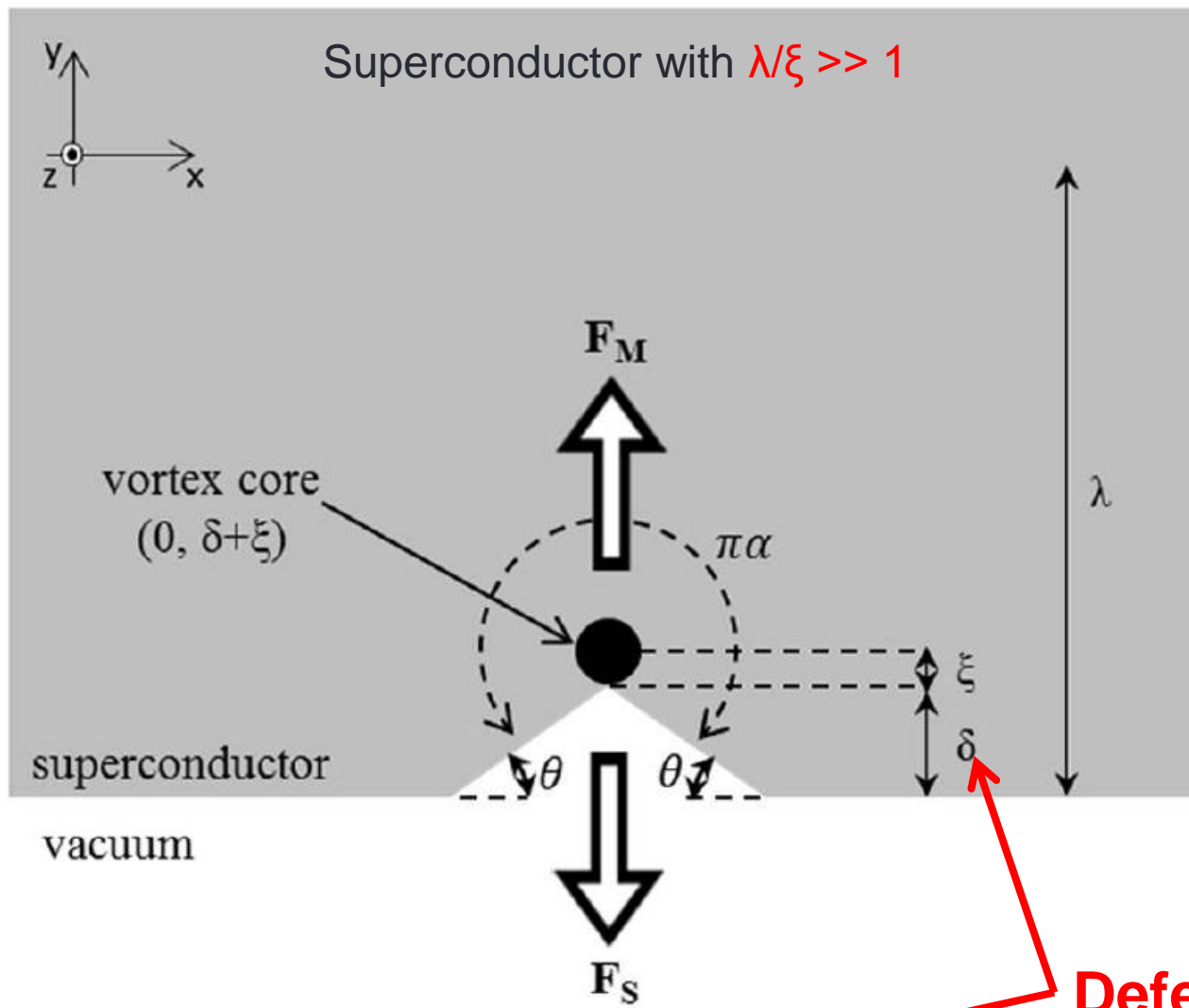
Surface is not ideally flat.

If we want to discuss the field limit, we should take existences of nano-defects into account and evaluate **the field at which Bean-Livingston barrier disappears.**
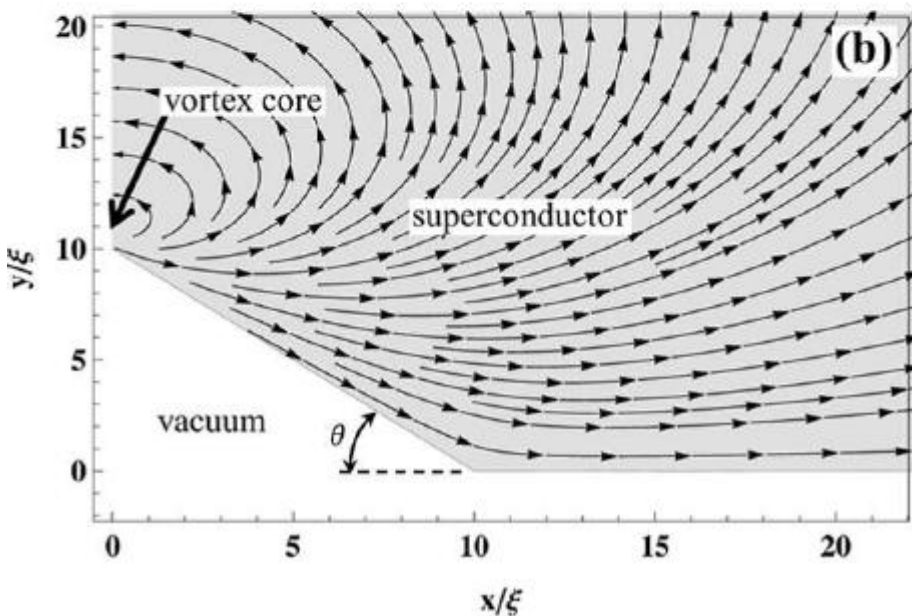
AFM image

SRF cavity surface after EP

Superconductor with a nano-scale groove

Nano-defect model
T. Kubo, LINAC14, 2014

C.Xu, H.Tian, C.Reece, and M.Kelley, Phys. Rev. ST Accel. Beams **14**, 123501 (2011)

Superconductor with $\lambda/\xi \gg 1$

vortex core $(0, \delta+\xi)$

$\mathbf{F_M}$

$\pi\alpha$

ξ

δ

λ

superconductor

θ　θ

vacuum

$\mathbf{F_S}$

Defect size

Assume $\xi \ll \delta \ll \lambda$

T. Kubo, LINAC14, 2014
T. Kubo, submitted to a journal

(a)

superconductor

vacuum θ

x/ξ

y/ξ
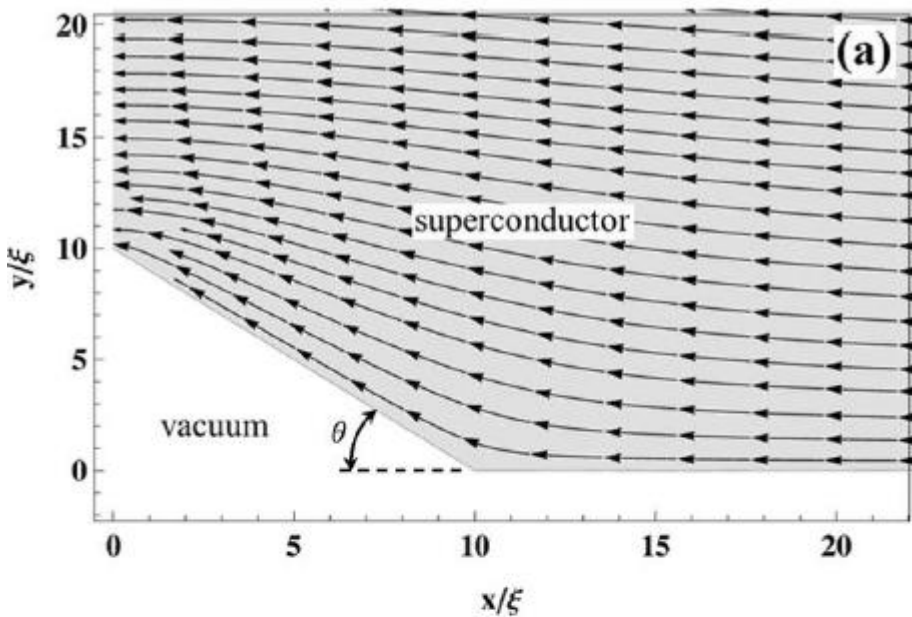
Can calculate
Screening current

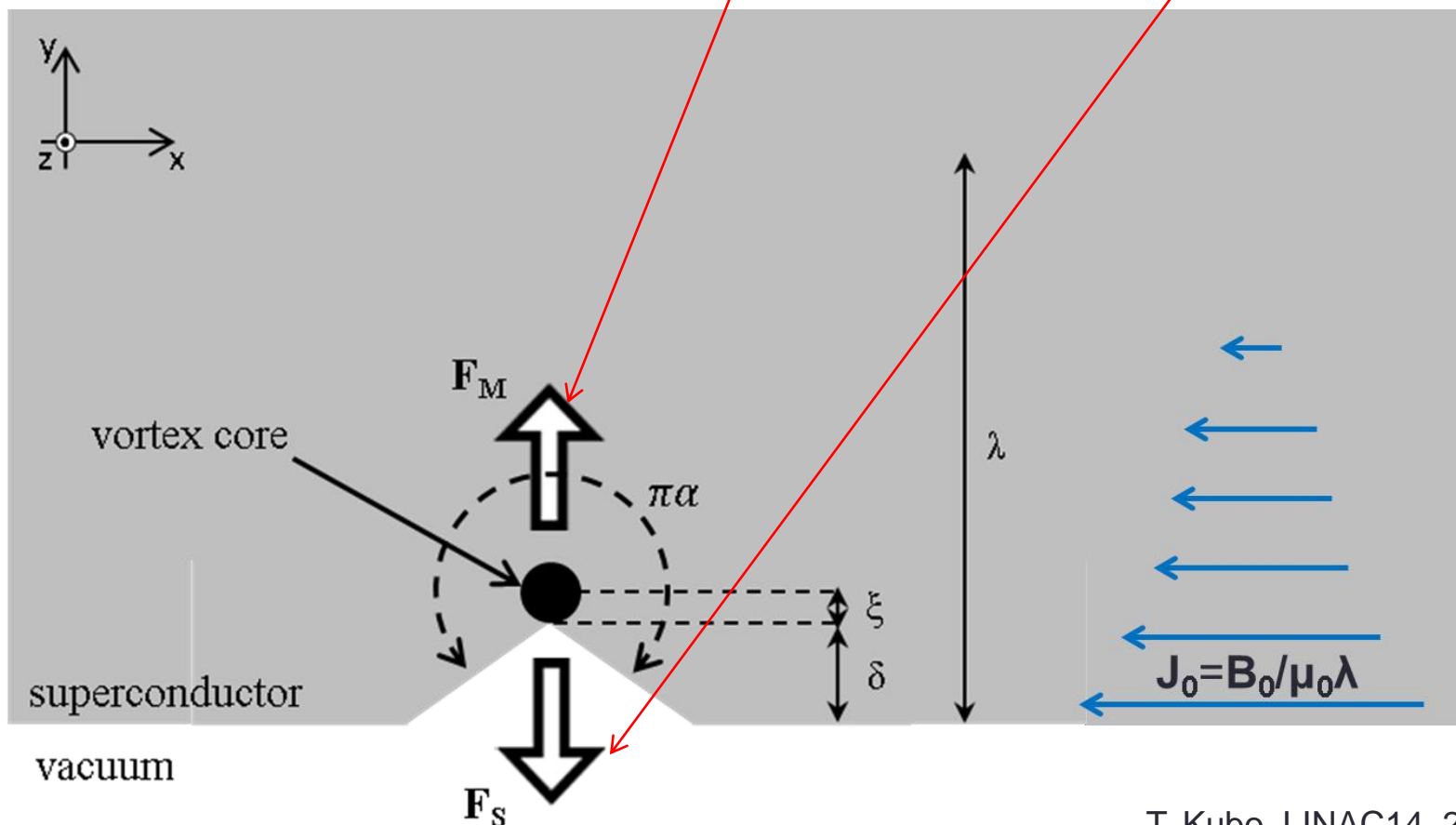$$J_{\mathrm{M}x}(x, y) - i J_{\mathrm{M}y}(x, y) = -\frac{J_0}{f(w)}\Big|_{w=F^{-1}(\zeta)}$$

J_0 is a screening current far from the groove, F^{-1} is the inverse of the map $F(w) = K_1 \int_0^w f(w')dw' + K_2$, $f(w) = w^{\alpha-1}(w^2-1)^{-\frac{\alpha-1}{2}}$, $K_1 = \sqrt{\pi}\delta/[\Gamma(\frac{\alpha}{2})\Gamma(\frac{3-\alpha}{2})\sin\frac{\pi(\alpha-1)}{2}]$, and $K_2 = i\delta$
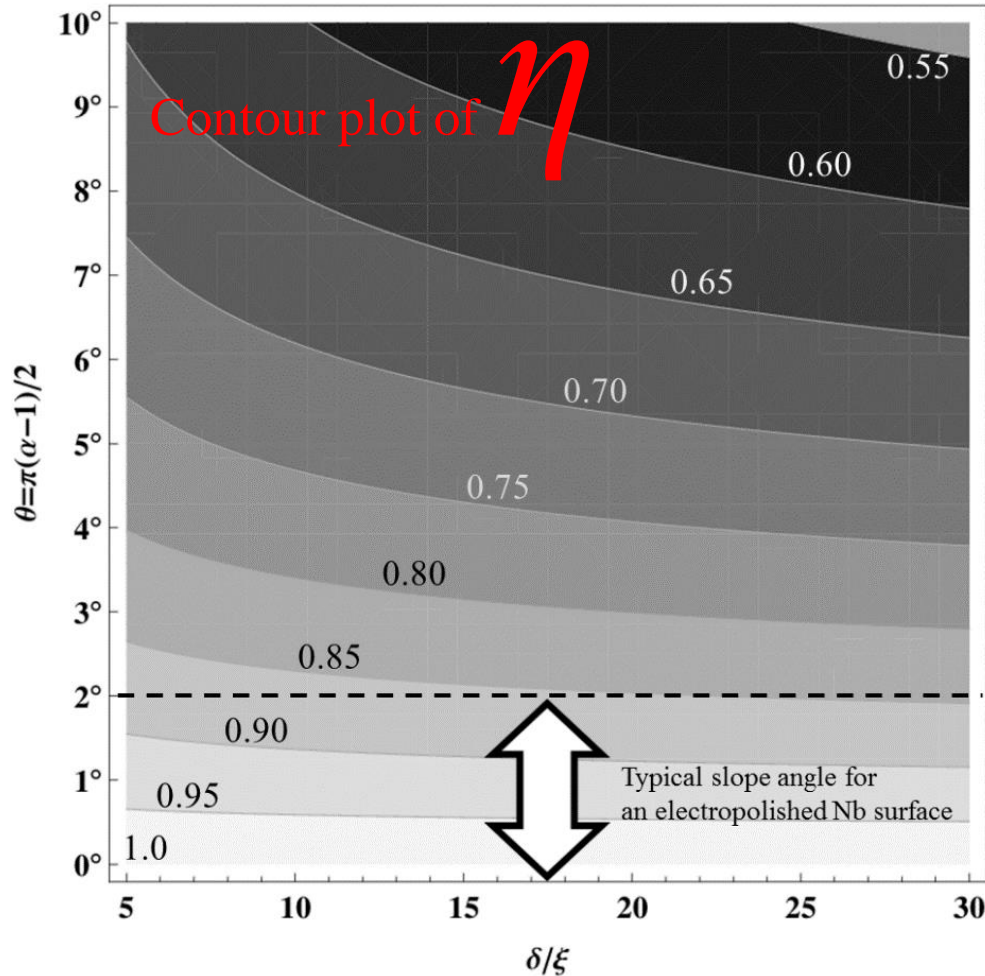

(b)

vortex core

superconductor

vacuum θ

x/ξ

y/ξ

and
Vortex current

$$J_{\mathrm{V+I}x}(x, y) - i J_{\mathrm{V+I}y}(x, y)$$
$$= \frac{1}{K_1 f(w)} \frac{-i\phi_0}{2\pi\mu_0\lambda^2}\left(\frac{1}{w - i\epsilon} - \frac{1}{w + i\epsilon}\right)\Big|_{w=F^{-1}(\zeta)}$$

T. Kubo, LINAC14, 2014
T. Kubo, submitted to a journal

Bean-Livingston barrier disappears when these two forces are balanced

$$\left(\frac{\sqrt{\pi}}{\Gamma(\frac{\alpha}{2})\Gamma(\frac{3-\alpha}{2})\alpha \sin \frac{\pi(\alpha-1)}{2}} \frac{\delta}{\xi} \right)^{\frac{\alpha-1}{\alpha}} \phi_0 \, J_0 = \frac{\phi_0^2}{4\pi\mu_0\lambda^2\xi\alpha} \, .$$

$J_0 = B_0/\mu_0\lambda$

T. Kubo, LINAC14, 2014
T. Kubo, submitted to a journal

$$\tilde{B}_s = \eta\, B_s \qquad \eta = \frac{1}{\alpha}\left(\frac{\Gamma(\frac{\alpha}{2})\Gamma(\frac{3-\alpha}{2})\alpha \sin\frac{\pi(\alpha-1)}{2}}{\sqrt{\pi}}\frac{\xi}{\delta}\right)^{\frac{\alpha-1}{\alpha}}$$

Contour plot of η

Typical slope angle for an electropolished Nb surface

Can evaluate a "suppression factor η" for materials such as
- Dirty Nb
- bulk Nb_3Sn
- multilayer NbN
- etc.

if you have data of surface topographic studies.

T. Kubo, LINAC14, 2014
T. Kubo, submitted to a journal

Immediate application:
Field limit of "Electropolsihed dirty Nb"

$$\tilde{B}_s = \eta\, B_s$$

$$\eta = \frac{1}{\alpha}\left(\frac{\Gamma(\frac{\alpha}{2})\Gamma(\frac{3-\alpha}{2})\alpha\sin\frac{\pi(\alpha-1)}{2}}{\sqrt{\pi}}\frac{\xi}{\delta}\right)^{\frac{\alpha-1}{\alpha}}$$

C.Xu, H.Tian, C.Reece, and M.Kelley,
Phys. Rev. ST Accel. Beams **14**, 123501 (2011)

BCP Surface Slope Histogram
EP Surface Slope Histogram

Surface after EP:
η ~ 0.9

T. Kubo, LINAC14, 2014
T. Kubo, submitted to a journal
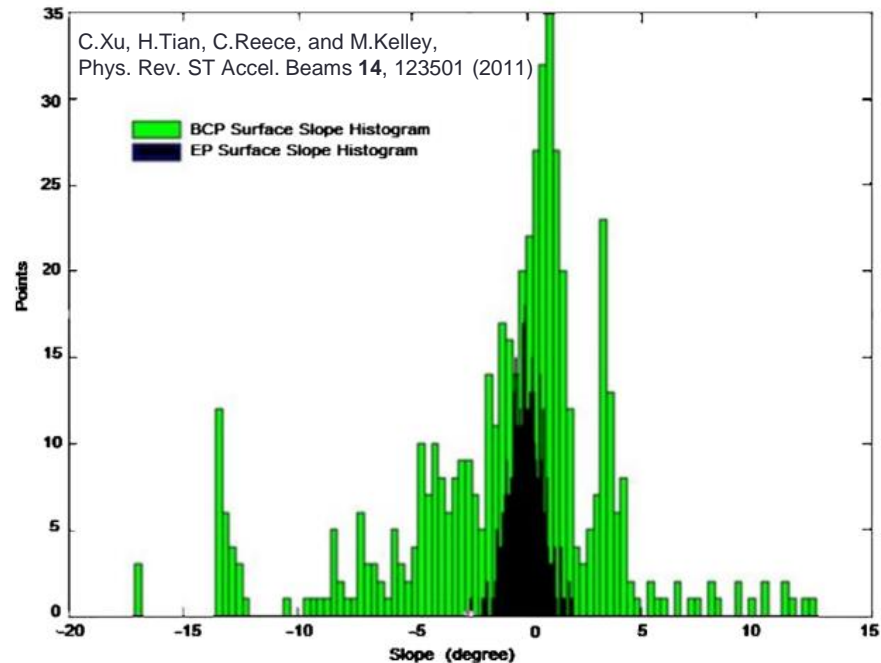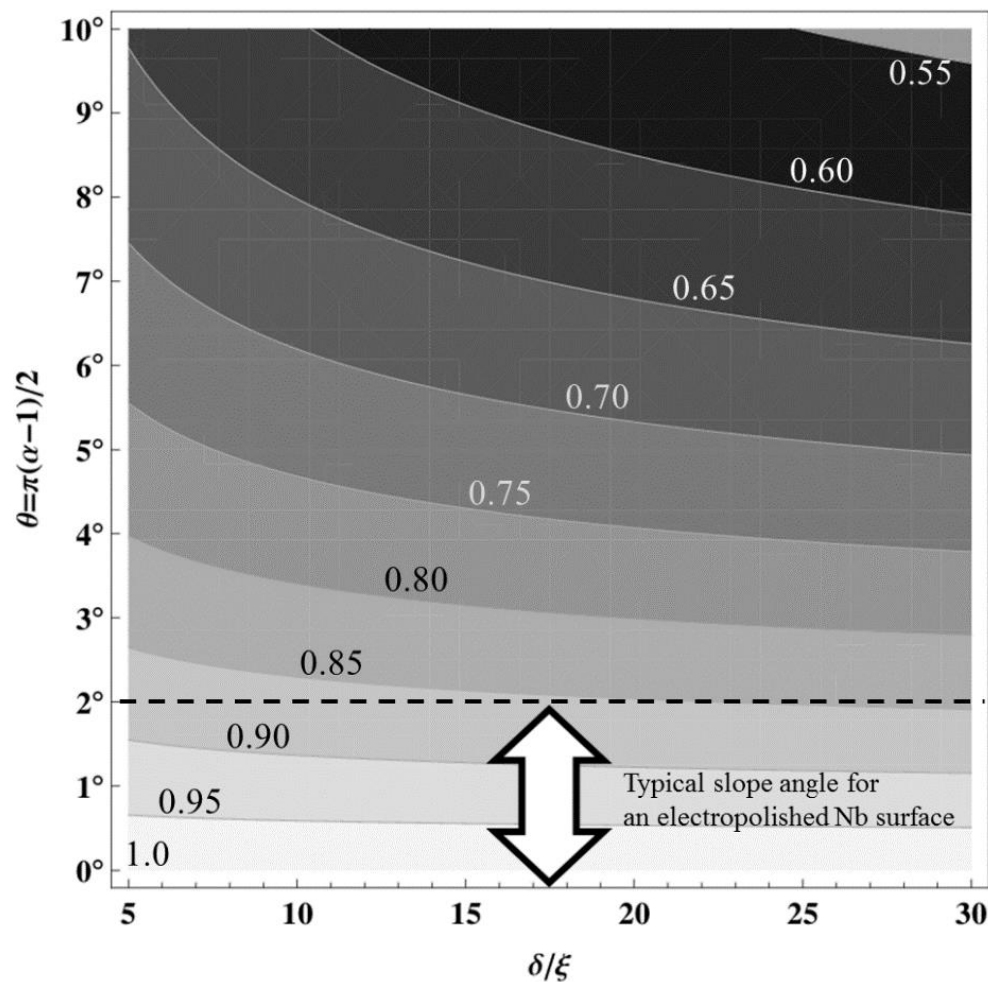
$$\tilde{B}_s = \eta\, B_s$$

$$\eta = \frac{1}{\alpha}\left(\frac{\Gamma(\frac{\alpha}{2})\Gamma(\frac{3-\alpha}{2})\alpha\sin\frac{\pi(\alpha-1)}{2}}{\sqrt{\pi}}\frac{\xi}{\delta}\right)^{\frac{\alpha-1}{\alpha}}$$
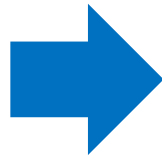
0.9   **$B_s = 0.71 B_c$**
(London theory)   ➡   **$\tilde{B}_s \sim 130\,mT$**

It is interesting to compare the above result with VT results of N-doped cavities. Each symbol corresponds to $(B_{pk}, Q_0) = $(achieved B_{pk}, Q_0 at achieved B_{pk}).

Good agreement with Record value

T. Kubo, 2014

$$\widetilde{B}_s = \eta \, B_s$$

$$\eta = \frac{1}{\alpha}\left(\frac{\Gamma(\frac{\alpha}{2})\Gamma(\frac{3-\alpha}{2})\alpha \sin\frac{\pi(\alpha-1)}{2}}{\sqrt{\pi}}\frac{\xi}{\delta}\right)^{\frac{\alpha-1}{\alpha}}$$
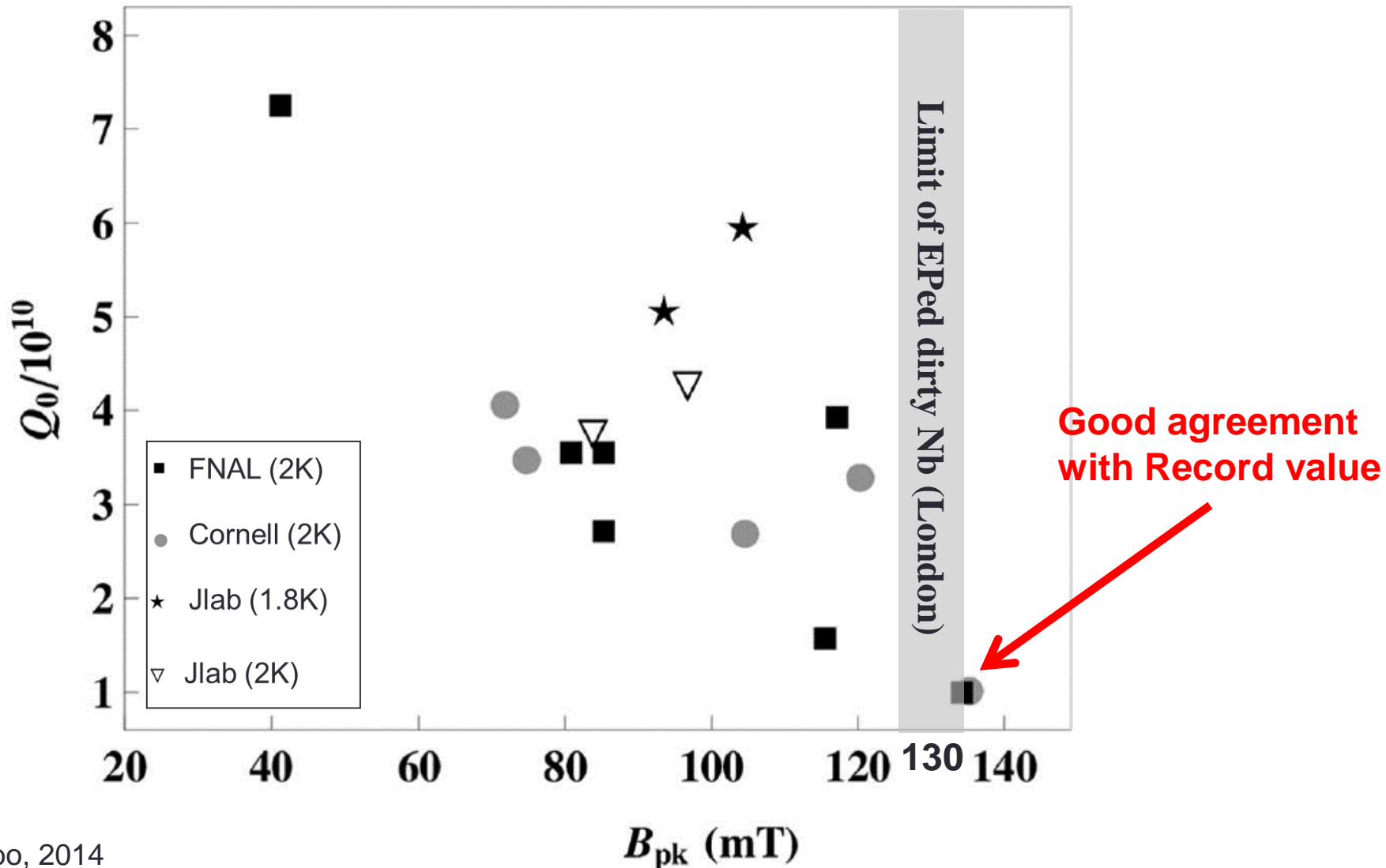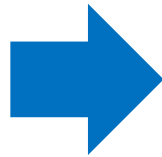
0.9

$B_s = 0.71 B_c$ ➡ $\widetilde{B}_s \sim 130\text{mT}$
(London theory)

extrapolate   London theory might underestimate

$B_s = 0.84 B_c$ ➡ $\widetilde{B}_s \sim 150\text{mT}$
(Quasi-classical theory)
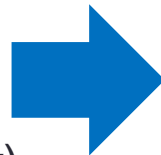
Catelani and Sethna, Phys. Rev. B **78**, 224509 (2008),
Lin, and Gurevich, Phys. Rev. B **85**, 054513 (2012).

It is interesting to compare the above result with VT results of N-doped cavities. Each symbol corresponds to $(B_{pk}, Q_0) = ($ achieved B_{pk}, Q_0 at achieved $B_{pk})$.

Due to the smallness of B_{c1}, vortices enter from $\eta < 0.9$ defect, if it exist.

Record value

Limit of dirty Nb with electroplished surface

Limit of dirty Nb with ideal flat surface

■ FNAL (2K)

● Cornell (2K)

★ Jlab (1.8K)

▽ Jlab (2K)

$Q_0/10^{10}$

B_{pk} (mT)

$\eta=0.5$

$\eta=0.9$

$\eta=1$

T. Kubo (2014)
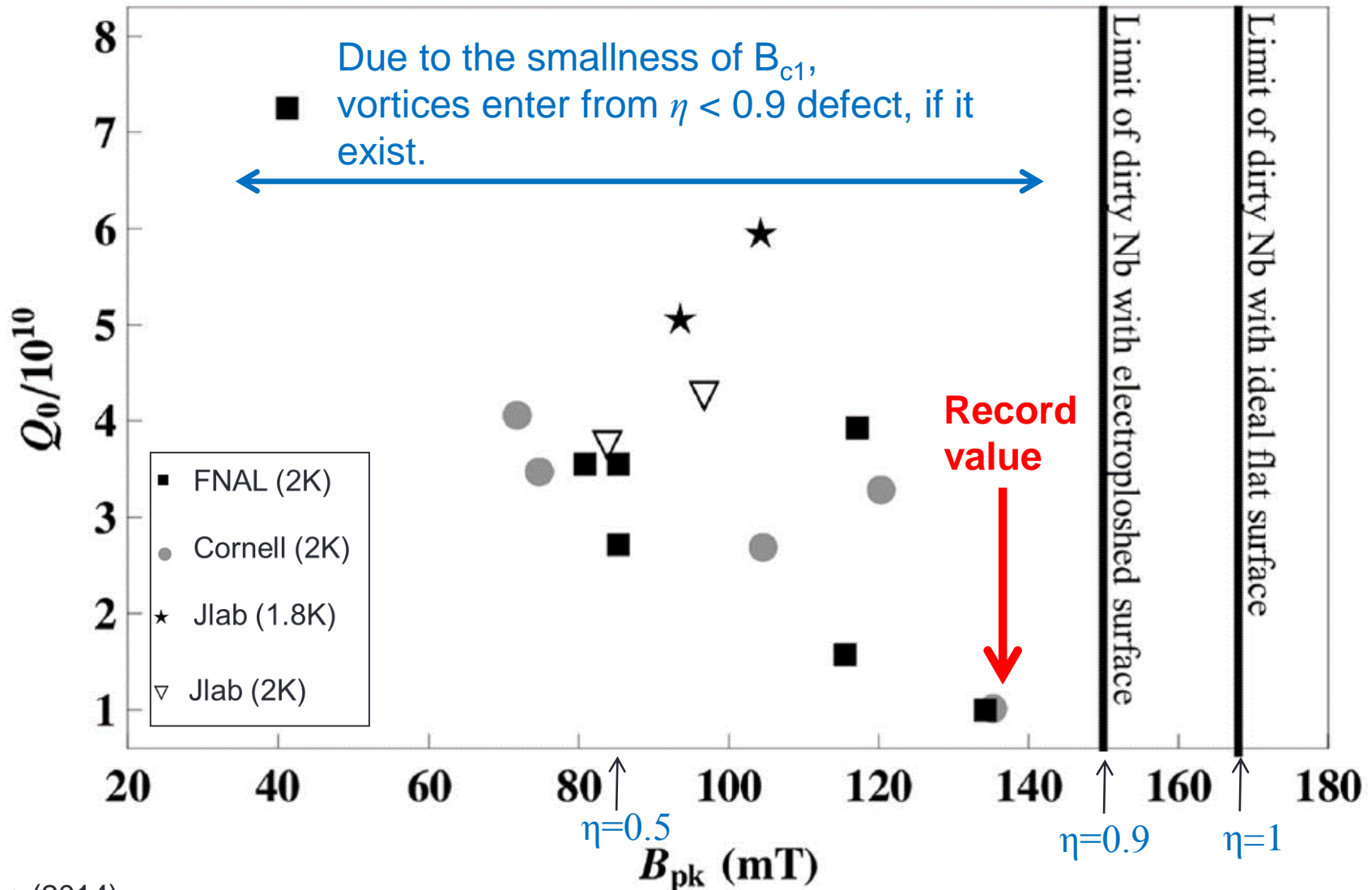
**I added an additional slide this morning.
Record value is updated: Charles's slide (p.10)**

RDT-13 180/20N/10 + 60 micron EP + 180/1N/60 + 10 micron EP
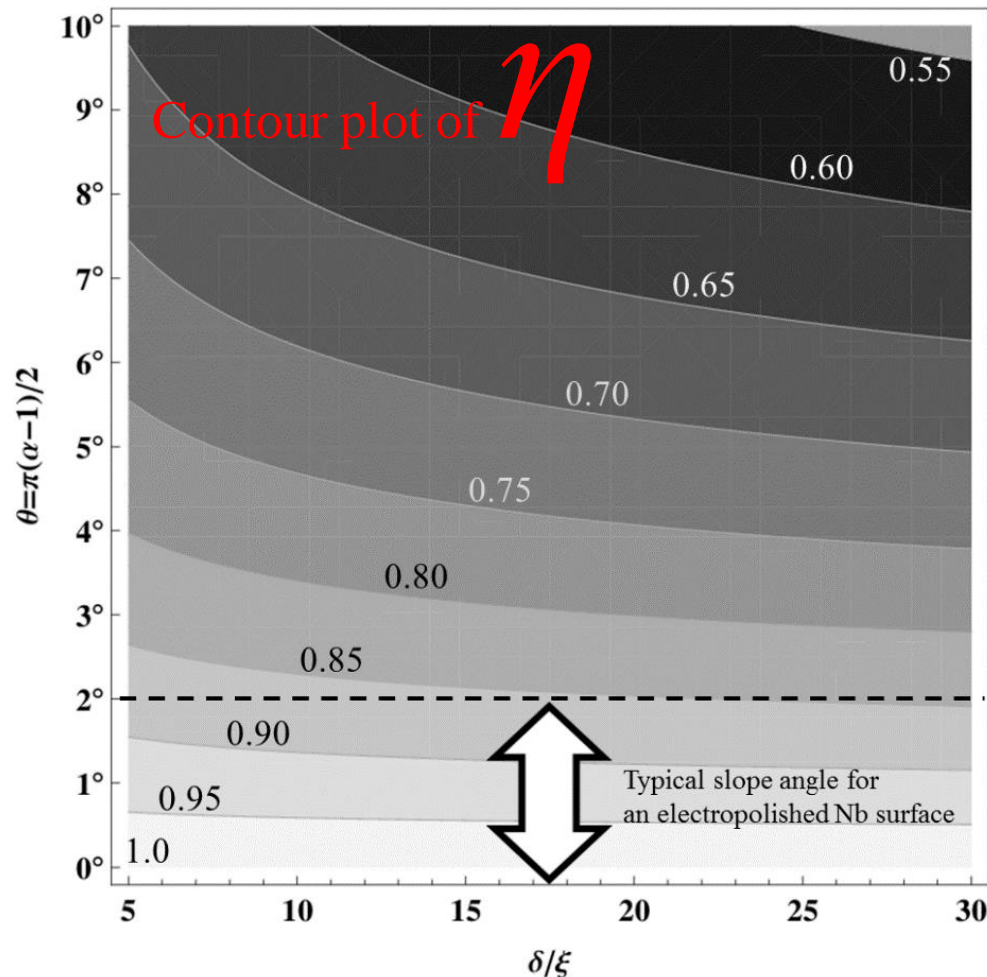
RDT-13, 25-Sep-14
Power limited @ 35 MV/m
T=2.0 K

Initial run prior to MP quenches

Qo

1.0E+10

1.0E+9

0.0   5.0   10.0   15.0   20.0   25.0   30.0   35.0   40.0

Eacc (MV/m)

Quite good agreement
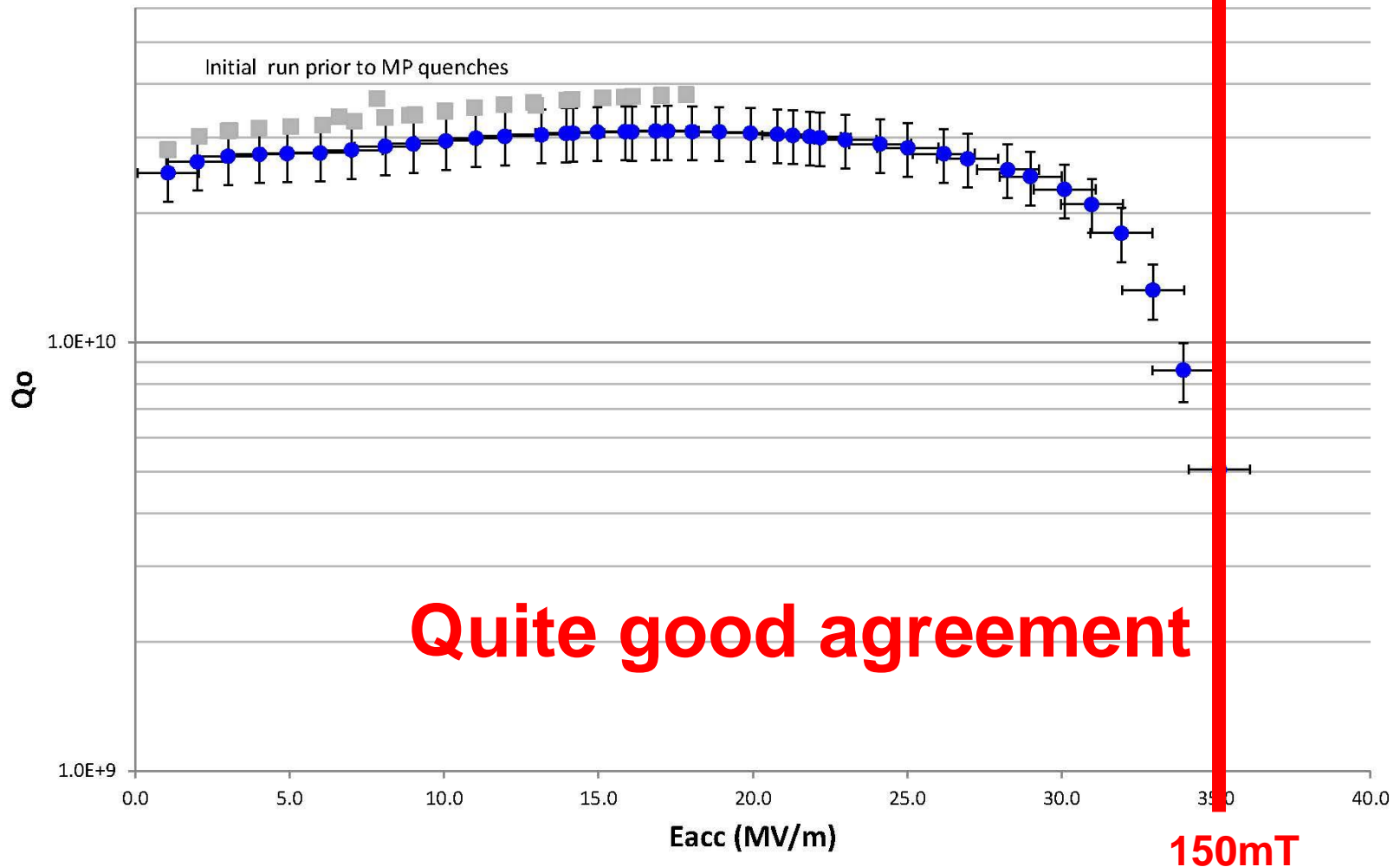
150mT

Comment on "immediate application"

- To achieve a field > 150mT or η > 0.9, smoother surface is necessary. Mechanical polishing technique that enables mirror-like finishes might be effective.

- 150mT corresponds to E_{acc}=35MV/m for TESLA cavity or E_{acc}=40MV/m for LSF cavity. Mirror-like finished and doped LSF cavity is a solution for ILC 1TeV upgrade?

$$\tilde{B}_s = \eta \, B_s \qquad \eta = \frac{1}{\alpha}\left(\frac{\Gamma(\frac{\alpha}{2})\Gamma(\frac{3-\alpha}{2})\alpha \sin\frac{\pi(\alpha-1)}{2}}{\sqrt{\pi}}\frac{\xi}{\delta} \right)^{\frac{\alpha-1}{\alpha}}$$

Contour plot of η

Typical slope angle for an electropolished Nb surface

Can evaluate a "suppression factor η" for materials such as
- Dirty Nb
- bulk Nb_3Sn
- multilayer NbN
- etc.

if you have data of surface topographic studies.

T. Kubo, LINAC14, 2014
T. Kubo, submitted to a journal

Supplement

When **B>B$_s$**, Bean-Livingston barrier disappears.
→ **Theoretical limit**
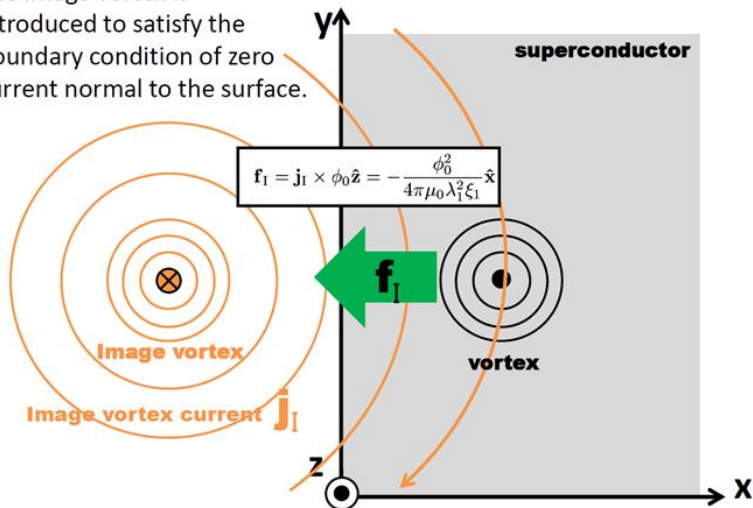
When **B>B$_{c1}$**, the stable position of a vortex is inside the SC, but Bean-Livingston barrier prevent vortex penetrations.

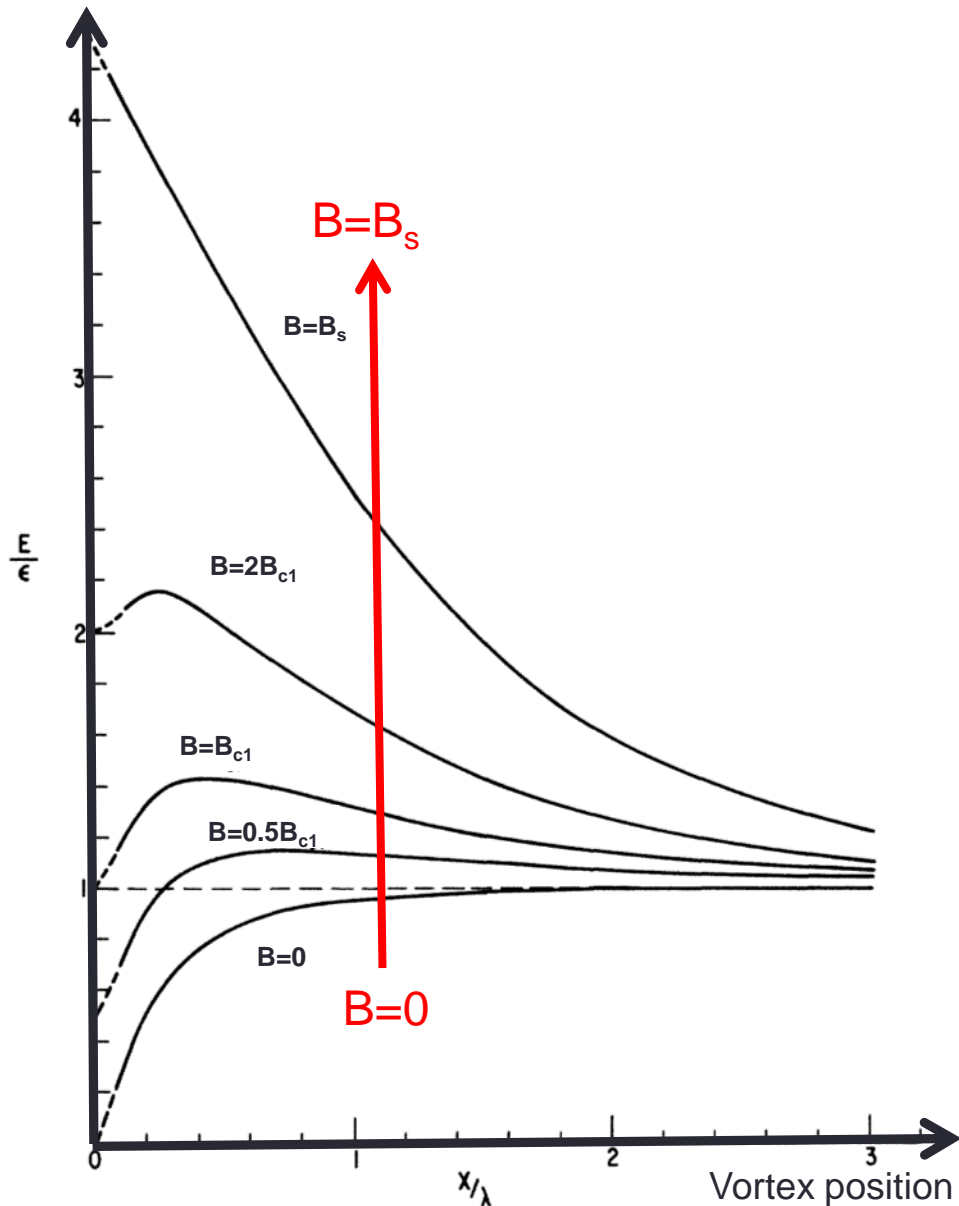When **B<B$_{c1}$**, there is no stable position inside the SC.

$B=B_s$

$B=2B_{c1}$

$B=B_{c1}$

$B=0.5B_{c1}$

$B=0$

$B=B_s$

$B=0$

$\frac{E}{\epsilon}$

x/λ

Vortex position

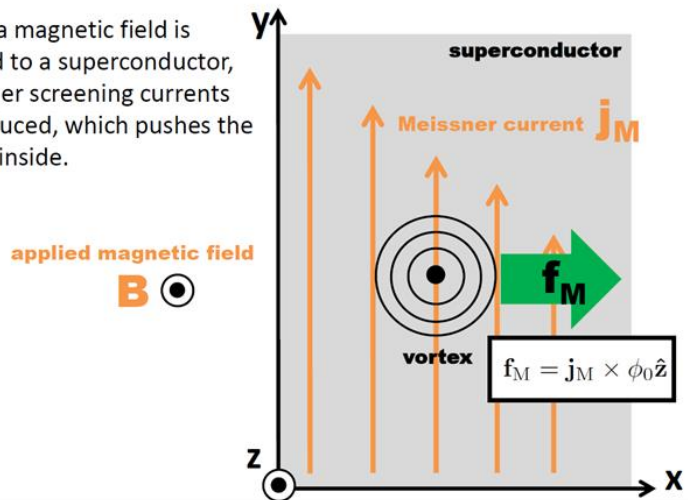C. P. Bean and J. D. Livingston, Phys. Rev. Lett. **12**, 14 (1964)
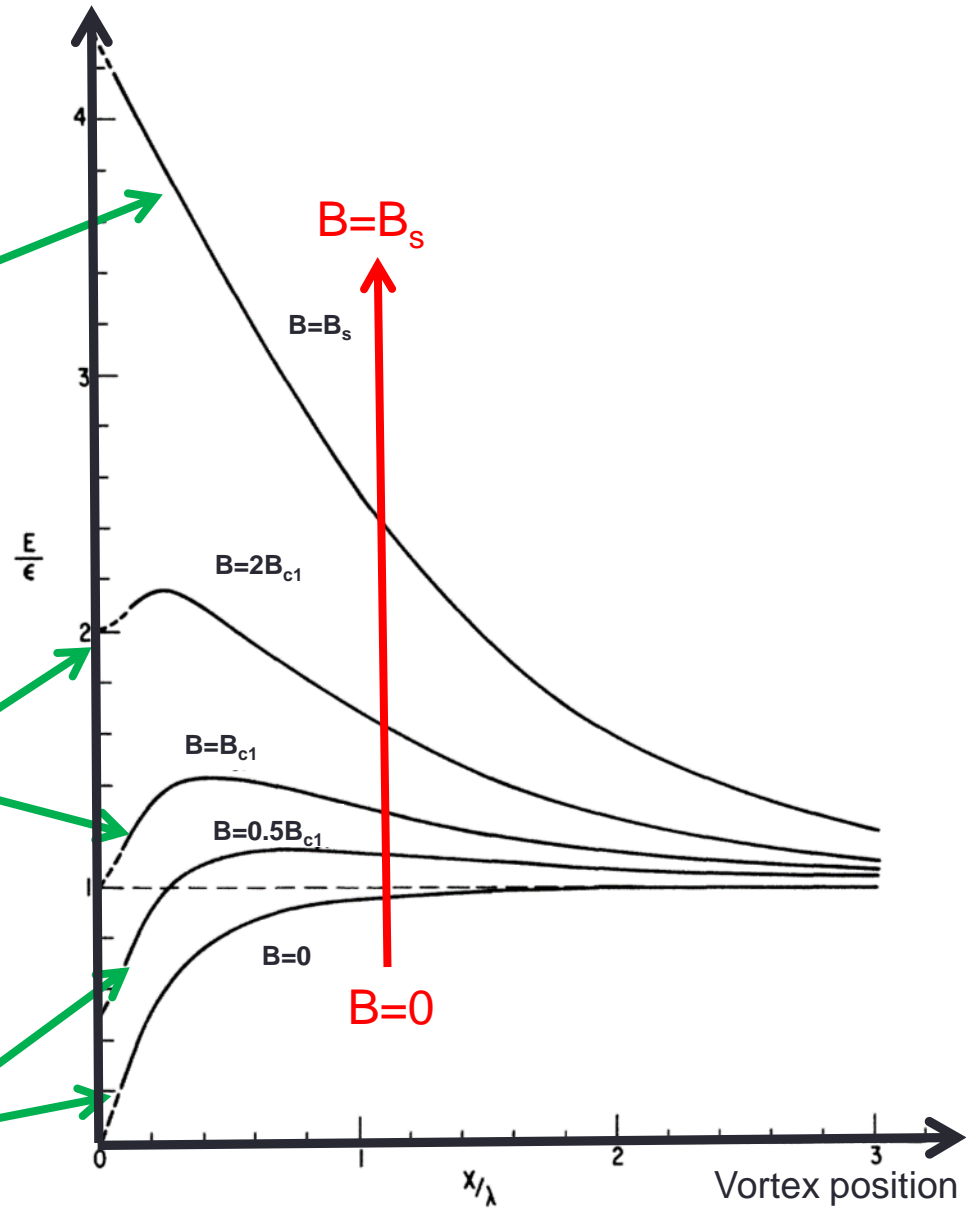
(a) Force from the image vortex

The image vortex is introduced to satisfy the boundary condition of zero current normal to the surface.

$$\mathbf{f}_I = \mathbf{j}_I \times \phi_0 \hat{\mathbf{z}} = -\frac{\phi_0^2}{4\pi\mu_0\lambda_1^2\xi_1}\hat{\mathbf{x}}$$

Image vortex

Image vortex current $\mathbf{j}_I$

superconductor

f_I

vortex

(b) Force from the external field
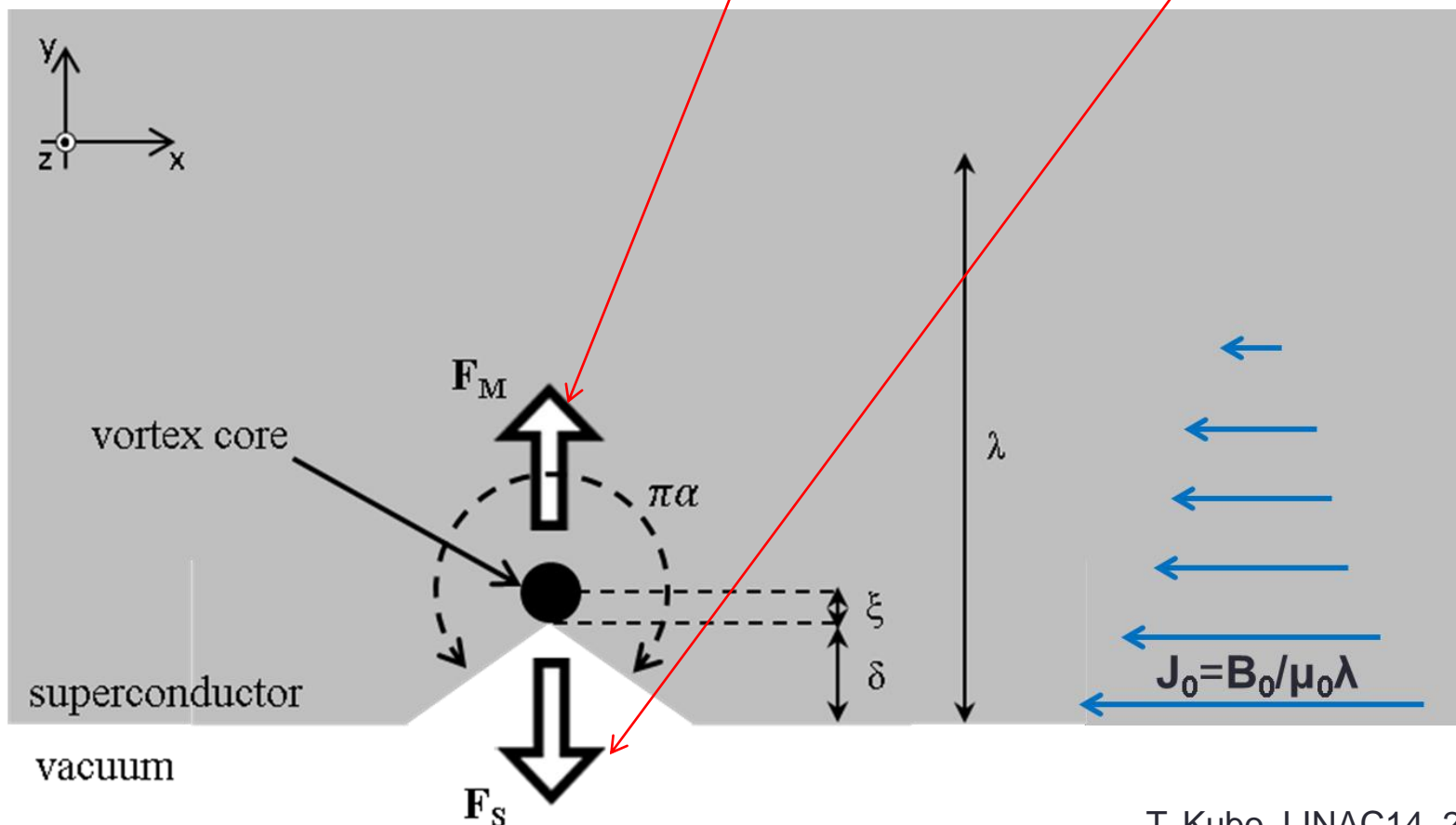
When a magnetic field is applied to a superconductor, Meissner screening currents are induced, which pushes the vortex inside.
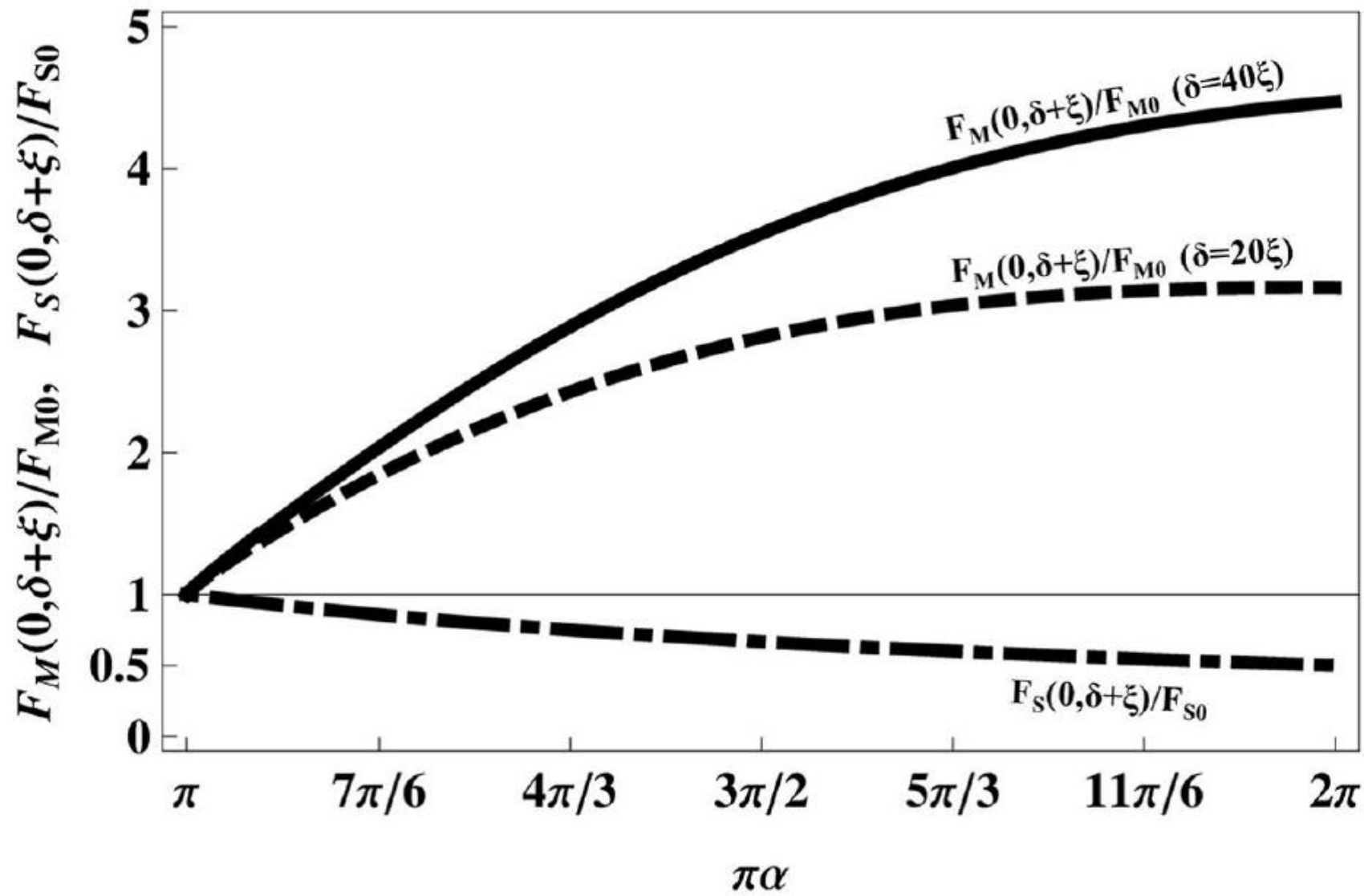
Meissner current $\mathbf{j}_M$

applied magnetic field

$\mathbf{B}$

vortex

f_M

superconductor

$$\mathbf{f}_M = \mathbf{j}_M \times \phi_0 \hat{\mathbf{z}}$$

T. Kubo, "Review on physics of the superconducting accelerating cavity and studies on electron-beam welding"
in proceedings of the 15th KEK Mechanical Engineering Workshop (2014), p. 14

$B=B_s$

$B=2B_{c1}$

$B=B_{c1}$

$B=0.5B_{c1}$

$B=0$

$\frac{E}{\epsilon}$

x/λ

Vortex position

C. P. Bean and J. D. Livingston, Phys. Rev. Lett. **12**, 14 (1964)

Bean-Livingston barrier disappears when these two forces are balanced

$$\left(\frac{\sqrt{\pi}}{\Gamma(\frac{\alpha}{2})\Gamma(\frac{3-\alpha}{2})\alpha\sin\frac{\pi(\alpha-1)}{2}}\frac{\delta}{\xi}\right)^{\frac{\alpha-1}{\alpha}}\phi_0\,J_0 = \frac{\phi_0^2}{4\pi\mu_0\lambda^2\xi\alpha}\,.$$

T. Kubo, LINAC14, 2014
T. Kubo, submitted to a journal

T. Kubo, LINAC14, 2014
T. Kubo, submitted to a journal

Previous study on "vortex-defect interaction"
A. Buzdin and M. Daumens, Physica C **294**, 257 (1998)

They consider "a groove with an infinite depth".
(misleading figures!)
A. Dzyuba, A. Romanenko and L. D. Cooley, Supercond. Sci. Technol. 23, 125011 (2010) also treat a groove with an infinite depth.
This model can not be applied to "nano-defect".
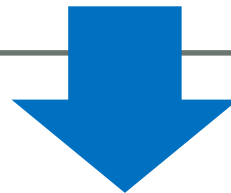
We must consider **"a groove with a depth smaller than the penetration depth".**
→ T. Kubo, LINAC14, TUPP071

T. Kubo, LINAC14, TUPP071, https://oraweb.cern.ch/pls/linac2014/TOC.htm

VORTEX-PENETRATION FIELD AT A GROOVE WITH A DEPTH SMALLER THAN THE PENETRATION DEPTH*

Takayuki Kubo†,

KEK, High Energy Accelerator Research Organization, Tsukuba, Ibaraki 305-0801, Japan

Abstract

Analytical formula to evaluate the vortex-penetration field at a groove with a depth smaller than penetration depth is derived, which can be applied to surfaces of cavities or test pieces made from extreme type II superconductors such as nitrogen-doped Nb or alternative materials like Nb_3Sn or NbN.

INTRODUCTION

The vortex-penetration field B_v is the field at which a vortex overcome the Bean-Livingston barrier [1] and start to penetrate into the superconductor (SC). B_v of extreme type II SC, where the penetration depth λ is much larger than the coherence length ξ, can be evaluated in the framework of the London theory. Materials that attract much attentions in the field of SC accelerating cavity such as dirty Nb like nitrogen-doped Nb and alternative materials like Nb_3Sn and NbN are all categorized into this class. For an SC with an ideal flat surface, B_v is given by $B_v = \phi_0/(4\pi\lambda\xi) \simeq 0.7 B_c$, where ϕ_0 is the flux quantum and B_c is the thermodynamic critical magnetic field. Actually, experiments shows fields can not reach such a level. More realistic assumption, such as surface irregularities, should be incorporated.

In this paper we consider a groove with a depth δ smaller than λ as a simple example of a surface irregularity, which assume irregularities on cavity surfaces or test pieces made from extreme type II SC such as a nitrogen-doped Nb or alternative materials. B_v at this type of irregularity has not been obtained so far, in spite of the fact that there are many studies on B_v at a surface irregularity [2, 3, 4, 5].

MODEL

Let us consider a groove shown in Fig. 1(a). Gray and white regions represent the SC and the vacuum, respectively. Surface, groove and applied magnetic-field are perpendicular to the x-y plane. The half width of the groove and the slope angle are given by R and $\pi(\alpha - 1)/2$, respectively, and thus the depth is given by $\delta = R\tan[\pi(\alpha-1)/2]$, where $1 < \alpha < 2$. The depth is assumed to satisfy $\xi \ll \delta \ll \lambda$.

FORCES ACTING ON A VORTEX AND THE VORTEX-PENETRATION FIELD

Suppose a vortex is at the position $(x, y) = (0, \delta + \xi)$, inside the bottom of groove. This vortex feels two distinct
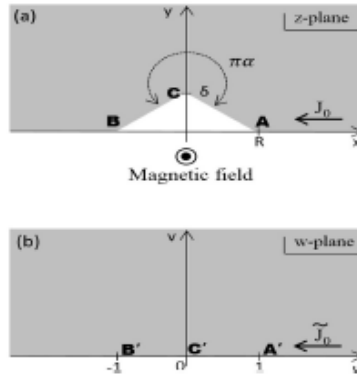
---

*The work is supported by JSPS Grant-in-Aid for Young Scientists (B), Number 26800157
† kuboaka@post.kek.jp

Figure 1: (a) Groove with a depth that is smaller than the penetration depth of the material and (b) its map on the w-plane.

forces: (i) F_M a force from a Meissner current due to an external field and (ii) F_I a force due to an image antivortex that is introduced to satisfy the boundary condition of zero current normal to the surface. The former and the latter draw the vortex to the inside and the outside of the SC, respectively. The vortex-penetration field is a field at which these competing forces are balanced. [1]

Force Due to an External Field

An external magnetic-field pushes a vortex into the superconductor by a force $F_M = J_M \times \phi_0\hat{z}$, where J_M is a Meissner screening-current, $\phi_0 = 2.07 \times 10^{-15}$ Wb is the flux quantum and $\hat{z}$ is the unit vector parallel to the z-axis. To evaluate F_M, we evaluate J_M as follows. J_M satisfies div $J_M = 0$ and one of the Maxwell equations, $J_M = $ rot H, where the magnetic field H plays the role of the vector potential of J_M. For our two-dimensional problem, H can be written as $H = (0, 0, -\psi(x, y))$, and J_M is given by $J_M = $ rot $H = (-\partial\psi/\partial y, \partial\psi/\partial x, 0)$. On the other hand, since λ is assumed to be much larger than the typical scale of the model, the London equation is reduced to rot $J_M = -\Delta H = 0$, which allows us to introduce a scalar potential of J_M. For our two-dimensional problem the scalar potential can be written as $\phi(x, y)$, and J_M is given by $J_M = -$grad $\phi = (-\partial\phi/\partial x, -\partial\phi/\partial y, 0)$. Since

[1] Detailed reviews are given in Ref. [6, 7].

---

both the two approaches should lead the same J_M, we find

$$J_{Mx} = -\frac{\partial\phi}{\partial x} = -\frac{\partial\psi}{\partial y}, \qquad J_{My} = -\frac{\partial\phi}{\partial y} = \frac{\partial\psi}{\partial x}, \quad (1)$$

which are the Cauchy-Riemann conditions. Thus a function defined by

$$\Phi_M(z) \equiv \phi(x, y) + i\psi(x, y), \quad (2)$$

is an holomorphic function of a complex variable $z = x + iy$, which is called the complex potential. If $\Phi_M(z)$ is given, components of J_M are derived from

$$J_{Mx} - iJ_{My} = -\frac{\partial\phi}{\partial x} + i\frac{\partial\phi}{\partial y} = -\frac{\partial\phi}{\partial x} - i\frac{\partial\psi}{\partial x} = -\frac{d\Phi_M(z)}{dz}, \quad (3)$$

where the property of the holomorphic function, $\Phi_M'(z) = \partial\phi/\partial x + i\partial\psi/\partial x$, is used. Thus our two-dimensional problem is reduced to a problem of finding $\Phi_M(z)$.

The complex potential $\Phi_M(z)$ is derived from a complex potential $\bar{\Phi}_M(w)$ on a complex w-plane shown in Fig. 1(b) through a conformal mapping $z = F(w)$, by which orthogonal sets of field lines in the w-plane are transformed into those in the z-plane. The map is given by the Schwarz-Christoffel transformation,

$$z = F(w) = K_1 \int_0^w f(w)dw + K_2. \quad (4)$$

The function $f(w)$ is given by

$$f(w) = w^{\alpha-1}(w^2 - 1)^{-\frac{\alpha-1}{2}}, \quad (5)$$

and the constants K_1 and K_2 are given by

$$K_1 = \frac{\sqrt{\pi}R}{\Gamma(\frac{\alpha}{2})\Gamma(\frac{3-\alpha}{2})\cos\frac{\pi(\alpha-1)}{2}}, \quad (6)$$

$$K_2 = i\delta = iR\tan\frac{\pi(\alpha-1)}{2}, \quad (7)$$

which are determined by conditions that A′ and C′ on the w-plane are mapped into A and C on the z-plane, respectively. The complex potential on the w-plane is given by $\bar{\Phi}_M(w) = \bar{J}_0 w$ ($\bar{J}_0 \equiv K_1 J_0$), which reproduces the current distribution on the w-plane: $-\bar{\Phi}_M'(w) = -\bar{J}_0$. Thus the complex potential on the z-plane is given by

$$\Phi_M(z) = \bar{\Phi}_M(F^{-1}(z)) = F^{-1}(z)\bar{J}_0, \quad (8)$$

where F^{-1} is an inverse function of F.

All that is left to do is to substitute Eq. (8) into Eq. (3). The we obtain

$$J_{Mx} - iJ_{My} = -\frac{J_0}{f(w)}, \quad (9)$$

where $dF^{-1}/dz = dw/dz = (dz/dw)^{-1} = (dF/dw)^{-1}$ is used. In order to evaluate J_M at the vortex position $z = z_v \equiv i(\delta + \xi)$, w corresponding to z_v is necessary. While no closed form of $w = F^{-1}(z)$ exist, that of an approximate

---

expression can be derived. Suppose $w = i\epsilon$ ($0 < \epsilon \ll 1$) is mapped into $z = z_v$ on the z-plane by Eq. (4). Then we obtain $i(\delta + \xi) \simeq i\delta + iK_1\epsilon^\alpha/\alpha$, and find a relation

$$\epsilon = \left(\frac{\alpha\xi}{K_1}\right)^{\frac{1}{\alpha}}, \quad (10)$$

which immediately leads

$$f(i\epsilon) \simeq \epsilon^{\alpha-1} = \left(\frac{\alpha\xi}{K_1}\right)^{\frac{\alpha-1}{\alpha}}. \quad (11)$$

Substituting Eq. (11) into Eq. (9), we find

$$J_{Mx}(z_v) = -\left(\frac{K_1}{\alpha\xi}\right)^{\frac{\alpha-1}{\alpha}}J_0, \qquad J_{My}(z_v) = 0. \quad (12)$$

Then the force due to the external field can be evaluated as

$$\mathbf{F}_M = \mathbf{J}_M \times \phi_0\hat{z}$$
$$= \left(\frac{\sqrt{\pi}}{\Gamma(\frac{\alpha}{2})\Gamma(\frac{3-\alpha}{2})\alpha\cos\frac{\pi(\alpha-1)}{2}}\frac{R}{\xi}\right)^{\frac{\alpha-1}{\alpha}}\phi_0 J_0\,\hat{y}, \quad (13)$$

where $\hat{y}$ is the unit vector parallel to the y-axis.

Force Due to the Image Antivortex

A current associated with a vortex near the surface satisfies the boundary condition of zero current normal to the surface. This boundary condition can be satisfied by removing the surface and introducing appropriate image antivortex (antivortices). Then the current can be expressed as $J_{v+I} = J_v + J_I$, where J_v and J_I represent currents due to the vortex and image antivortex (antivortices), respectively. The force due to the image antivortex (antivortices) F_I is given by $F_I = J_I \times \phi_0\hat{z}$. Thus our next task is to evaluate J_I at the vortex position $z = z_v \equiv i(\delta + \xi)$.

A scalar and a vector potentials of J_{v+I}, and the complex potential Φ_{v+I} can be introduced in much the same way as the above. Then components of J_{v+I} are given by

$$J_{V+Ix} - iJ_{V+Iy} = -\frac{d\Phi_{V+I}(z)}{dz}, \quad (14)$$

where $\Phi_{V+I}(z)$ can be derived from the complex potential $\bar{\Phi}_{V+I}(w)$ on the w-plane. Since the vortex and the image antivortex on the w-plane are located at $w = +i\epsilon$ and $-i\epsilon$, respectively, $\bar{\Phi}_{V+I}(w)$ is given by

$$\bar{\Phi}_{V+I}(w) = \frac{i\phi_0}{2\pi\mu_0\lambda^2}[\log(w - i\epsilon) - \log(w + i\epsilon)], \quad (15)$$

and thus the complex potential on the z-plane is given by

$$\Phi_{V+I}(z) = \bar{\Phi}_{V+I}(F^{-1}(z)). \quad (16)$$

F is the Schwarz-Christoffel transformation given by Eq. (4). Substituting Eq. (16) into Eq. (14), we find

$$J_{V+Ix} - iJ_{V+Iy} = \frac{1}{K_1 f(w)}\frac{-i\phi_0}{2\pi\mu_0\lambda^2}\left(\frac{1}{w - i\epsilon} - \frac{1}{w + i\epsilon}\right). \quad (17)$$

At the vortex position $z = z_v$ or $w = i\epsilon$, the first term of the square bracket diverges, which is contribution from the current due to the vortex and should be abandoned for the computation of J_1. Then J_1 at the vortex position is give by

$$J_{1x} - iJ_{1y} = \frac{1}{K_1 f(i\epsilon)} \frac{i\phi_0}{2\pi\mu_0\lambda^2}\left(\frac{1}{2i\epsilon}\right) = \frac{\phi_0}{4\pi\mu_0\lambda^2\xi\alpha}, \quad (18)$$

or,

$$J_{1x}(z_v) = \frac{\phi_0}{4\pi\mu_0\lambda^2\xi\alpha}, \qquad J_{1y}(z_v) = 0, \quad (19)$$

where a relation $\epsilon f(i\epsilon) = \epsilon^\alpha = \alpha\xi/K_1$ is used. Then the force due to the image anti-vortex is given by

$$\mathbf{F}_1 = \mathbf{J}_M \times \phi_0\hat{a} = -\frac{\phi_0^2}{4\pi\mu_0\lambda^2\xi\alpha}\hat{\mathbf{y}}. \quad (20)$$

Note that Eq. (20) is reduced to the force from the flat surface when $\alpha = 1$, and is maximized when the groove is a crack with $\alpha \simeq 2$. Eq. (20) is identical with that given in Ref. [3].

Vortex-penetration field

The vortex-penetration field B_v can be evaluated by balancing the two competing forces given by Eq. (13) and (20):

$$\left(\frac{\sqrt{\pi}}{\Gamma(\frac{\alpha}{2})\Gamma(\frac{3-\alpha}{2})\alpha\cos\frac{\pi(\alpha-1)}{2}}\frac{R}{\xi}\right)^{\frac{\alpha-1}{\alpha}}\phi_0 J_0 = \frac{\phi_0^2}{4\pi\mu_0\lambda^2\xi\alpha}. \quad (21)$$

The surface current J_0 is given by $J_0 = -\mu_0^{-1}dB/dx|_{x=0} = B_0/\mu_0\Lambda$, where B_0 is the surface magnetic-field and Λ is a quantity with the dimension of length. For examples,

$$\Lambda = \begin{cases} \lambda & (\text{semi-infinite SC}), \\ \lambda\frac{\cosh\frac{d_S}{\lambda} + (\frac{\lambda'}{\lambda} + \frac{d_I}{\lambda})\sinh\frac{d_S}{\lambda}}{\sinh\frac{d_S}{\lambda} + (\frac{\lambda'}{\lambda} + \frac{d_I}{\lambda})\cosh\frac{d_S}{\lambda}} & (\text{multilayer SC}). \end{cases} \quad (22)$$

where d_S, d_I, and λ' are an SC layer thickness, insulator layer thickness and penetration depth of SC substrate material, respectively.[2] The finally we obtain

$$B_v = \frac{\phi_0}{4\pi\lambda\xi}\frac{\Lambda}{\lambda}\frac{1}{\alpha}\left(\frac{\Gamma(\frac{\alpha}{2})\Gamma(\frac{3-\alpha}{2})\alpha\cos\frac{\pi(\alpha-1)}{2}}{\sqrt{\pi}}\frac{\xi}{R}\right)^{\frac{\alpha-1}{\alpha}}, \quad (23)$$

Note that Eq. (23) is reduced to B_v of semi-infinite SC or multilayer SC with ideal flat-surface when $\alpha = 1$.

SUMMARY

Analytical formula to evaluate the vortex-penetration field at a groove with a depth smaller than penetration depth was derived. The formula would be useful to analyze relation between surfaces and performance-test results of cavities or test pieces made from extreme type II SC such as a dirty Nb like nitrogen-doped Nb or alternative materials like Nb_3Sn or NbN.

REFERENCES

[1] C. P. Bean and J. D. Livingston, Phys. Rev. Lett. **12**, 14 (1964).

[2] F. Bass, V. D. Freilikher, B. Ya. Shapiro, and M. Shvartser, Physica C **260**, 231 (1996).

[3] A. Buzdin and M. Daumens, Physica C **294**, 257 (1998).

[4] A. Buzdin and M. Daumens, Physica C **332**, 108 (2000).

[5] A. Yu. Aladyshkin, A. S. Mel'nikov, I. A. Shereshevsky, and I. D. Tokman, Physica C **361**, 67 (2001).

[6] T. Kubo, Y. Iwashita, and T. Saeki, in *Proceedings of SRF2013, Paris, France* (2013), p. 427, TUP007.

[7] T. Kubo, Y. Iwashita, and T. Saeki, in *Proceedings of IPAC'14, Dresden, Germany* (2014), p. 2522, WEPRI023.

[8] A. Gurevich, Appl. Phys. Lett. **88**, 012511 (2006).

[9] T. Kubo, Y. Iwashita, and T. Saeki, Appl. Phys. Lett. **104**, 032603 (2014).

[10] T. Kubo, Y. Iwashita, and T. Saeki, in *Proceedings of IPAC'13, Shanghai, China* (2013), p. 2343, WEPWO014.

Formulae for semi-infinite SC and multilayer SC.
See also the reference T. Kubo, Y. Iwashita, T. Saeki, Appl. Phys. Lett. **104**, 032603 (2014) for the multilayer SC.

[2] See Ref. [8, 9]. Detailed reviews are given in Ref. [6, 7, 10].